Final Report of the INFUSE grant (CRADA 2706) between PPPL and Tokamak Energy, "Investigating microstability characteristics of next step tokamaks across a range of aspect ratios"

Report Date: April 26, 2024

In accordance with Requirements set forth in the terms of the CRADA, this document is the CRADA Final Report, including a list of Subject Inventions. It is to be forwarded to the DOE Office of Scientific and Technical Information upon completion or termination of the CRADA, as part of the commitment to the public to demonstrate results of federally funded research.

Parties to the Agreement: The Trustees of Princeton University under its U.S. Department of Energy Contract No. DE-AC02-09CH11466, and Tokamak Energy, Inc.

CRADA number: 2706

CRADA Title: Investigating microstability characteristics of next step tokamaks across a range of aspect ratios

Responsible Technical Contact at DOE Lab: John W. Berkery, Princeton Plasma Physics Laboratory

Name and Email Address of POC at Company: Michele Romanelli, Michele.Romanelli@tokamakenergy.co.uk

Sponsoring DOE Program Office(s): Fusion Energy Sciences

Executive Summary of CRADA Work

Researchers from PPPL partnered with Tokamak Energy to assess their preliminary design of a next step spherical tokamak, ST-E1. First plasma equilibria were developed with a range of aspect ratios and magnetic field strengths, with more peaked or more flat density profiles. Profiles were chosen to be stable to infinite-*n* ballooning stability, as determined by BALOO and ballstab. With M3D-C1 it was seen that the candidate equilibrium was MHD stable to $n = 1$ to 9 modes, and only unstable when Bateman-scaled down to 0.44. A radiated power assessment also found that on the order of 10 MW of power could be radiated, depending on impurity assumptions. In the area of microscopic stability, gyrokinetic stability was evaluated across shaping and aspect-ratio. Infinite-n ballooning stable equilibria were prepared and gyrokinetic codes CGYRO and GS2 were used to find growth rates of various other modes across a range of binormal wavenumbers and plasma radii in the core. Higher triangularity, squareness, toroidal field, and aspect-ratio were all predicted to drive higher transport across all wavenumbers and modes, with the exception of the Kinetic ballooning mode (KBM). The transport codes TGYRO and TRINITY were coupled with gyrokinetic codes CGYRO and GX and neoclassical models to calculate the self-consistent profiles, equilibrium, and heating profiles across triangularity, squareness, toroidal field, and aspect-ratio. Finally, an intriguing feature of the scan was noticed and further explored: that total fusion power could be controlled by adjusting the plasma volume fraction that is packed into power dense regions, primarily by using squareness as an actuator. This research has been submitted as a journal paper and the wider gyrokinetic work is being prepared for submission as well.

Introduction

In August of 2020 an INFUSE award was enacted between Tokamak Energy (TE) in the UK and the Princeton Plasma Physics Laboratory (PPPL) in the US for collaborative research on investigating microstability characteristics of next step tokamaks across a range of aspect ratios (https://infuse.ornl.gov/awards/investigating-microstability-characteristics-of-next-step-tokamaks-across-a-range-of-aspect-ratios/). Unfortunately, due to delays in enacting the agreement and then a change in the PPPL principal investigator due to the original PI leaving, work did not begin on this award until 2023. It was extended in April of 2023 to an end date of April 26, 2024.

The objective of this project was to investigate how turbulent transport characteristics change as a function of key device parameters in tokamaks, namely, aspect ratio and plasma beta, especially at reactor scales and magnetic field strengths. While the extended NSTX energy confinement time scaling provides a useful indication of the target parameter space for next step high field spherical tokamaks (STs), there is uncertainty over the parameter range in which the scaling is valid. Further, there remain open questions as to the optimal combination of aspect ratio and beta/toroidal field that will minimize turbulent losses at reactor scale specifically, at low-A and high-β. This project proposed to begin addressing these questions through the use of gyrokinetic simulations to provide valuable understanding that will be used to optimize the design of Tokamak Energy's planned device, ST-E1, along with other proposed next step tokamaks.

First, a systems code followed by a 1.5D transport code was used to produce plasma equilibria and kinetic profiles that satisfy a set of high-level criteria across a range of aspect ratios. These equilibria were subjected to various stability and radiated power analyses. Finally, linear gyrokinetic simulations was used to characterize the strength and thresholds of micro-instabilities across the range of target equilibria to identify which configurations are most likely to project to high confinement.

Develop plasma equilibria for a range of aspect ratios

This work was performed primarily by Alsu Sladkomedova and Salomon Janhunen from Tokamak Energy.

A series of Grad-Shafranov plasma equilibrium was produced that satisfied a set of high-level criteria (fusion power, device geometry, engineering considerations, stability limits, etc.). A systems code was used to determine consistent zero-dimensional plasma operating points at a range of aspect ratios that satisfy the criteria. To generate the self-consistent Grad-Shafranov equilibrium and set of kinetic profiles (ion and electron densities and temperatures) required for further analysis, the global parameters determined in the system code study were then used as the input to a 1.5D (1D profiles as a function of a magnetic flux coordinate + a 2D Grad-Shafranov equilibrium) transport code, ASTRA.

To perform these transport simulations additional assumptions were made. The electron density profile was prescribed, and ion and electron heat diffusivities were prescribed so that the direct problem was solved for ion and electron temperatures. The absolute values of heat diffusivities were set so Q=20 and the fusion power = 400 MW.

To facilitate straightforward data transfer from ASTRA to the other codes subsequently used in this project the ASTRA output was run through the CHEASE code to recompute the magnetic equilibrium from the p' and ff' profiles, and output in the EFIT data format.

Initial equilibria

An initial iteration between TE and PPPL to find ideal infinite n ballooning stable profiles (described in the next section) resulted in two cases: RUN2 with lower temperature gradient but higher density gradient, and RUN4 with higher temperature gradient but lower density gradient. Both have the same prescribed fusion power. Figure 1 shows the RUN2 equilibrium, as an example.

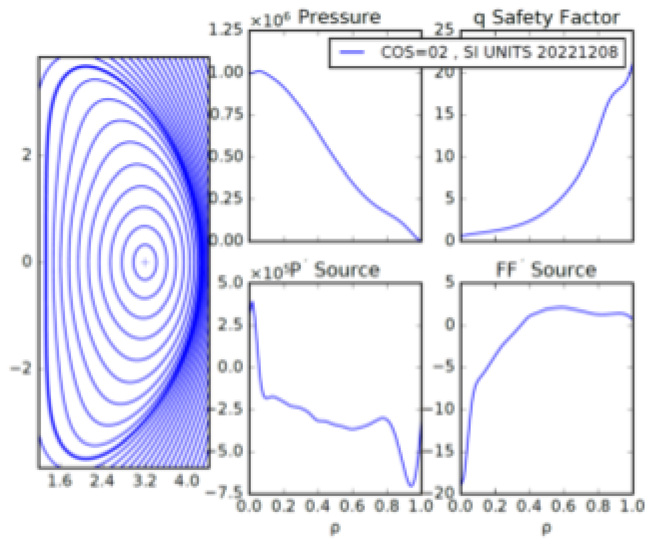

Figure 1: example equilibrium reconstruction (RUN2) for ST-E1.

Equilibrium scans

A series of equilibrium scans was then performed, of aspect ratio A, and toroidal field B_T, for both a more peaked and flatter density profile. These are summarized in Fig. 2, with safety factor, q, plots indicating that all the runs have $q > 3$. These plasmas have 90% of bootstrap current and densities just below the Greenwald limit. The high safety factor on-axis is due to a low bootstrap current fraction in the core and low residual Ohmic current. The Ohmic current that was still present can be regarded as an external current drive. For the toroidal magnetic field scan, only the input B_T was changed. For the aspect ratio scan, the input heating power was scaled accordingly with an increase in the plasma volume. Note that the density and temperature profiles are identical in all cases. Since the volume increases with aspect ratio, the volume averaged electron density and temperature are lower at higher A.

Finally, RUN22 was generated as a repeat of RUN8 with additional current in the core to flatten the q profile, as well as an imposed x-point geometry. This RUN22 was the basis of much of the further work in this project.

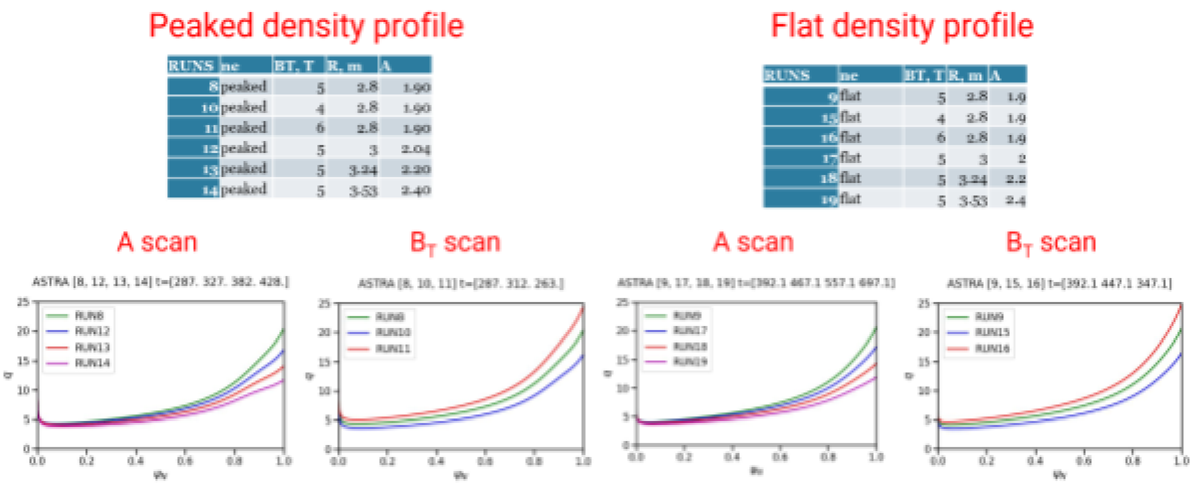

RUNS	ne	BT, T	R, m	A
8	peaked	5	2.8	1.90
10	peaked	4	2.8	1.90
11	peaked	6	2.8	1.90
12	peaked	5	3	2.04
13	peaked	5	3.24	2.20
14	peaked	5	3.53	2.40

RUNS	ne	BT, T	R, m	A
9	flat	5	2.8	1.9
15	flat	4	2.8	1.9
16	flat	6	2.8	1.9
17	flat	5	3	2
18	flat	5	3.24	2.2
19	flat	5	3.53	2.4

Figure 2: equilibrium reconstruction scans for ST-E1.

Macroscopic stability assessment

This work was performed primarily by Jack Berkery and Steve Jardin from PPPL.

Once the equilibria have been generated, a first step is to assess their macro stability against various MHD modes. The goal outlined in the proposal was that the equilibrium should remain below the no wall normalized beta threshold. Candidate modes to assess also generally included internal or global kink modes and infinite *n* ballooning modes.

Infinite-n ballooning stability

For the RUN2 initial equilibrium, the profiles were chosen to be just at the infinite-*n* ballooning stability threshold. This can be seen in Fig. 3 which includes a plot (left) from the BALOO code of the "experimental" α profile vs. normalized poloidal flux, where α is a normalized pressure gradient term. The profile falls under the unstable region. On the right are plots made with the ballstab code (a module of GS2) which shows the stability space in s (= $(r/q)(dq/dr)$) vs. $-d\beta/d(r/a)$, which is related to α, for particular Ψ_N surfaces. Note a scale change in the two ballstab plots. In a similar assessment of the RUN22 equilibrium shown in Fig. 4, no unstable region was found by BALOO and indeed ballstab found the two surfaces tested to be well below the unstable region in s.

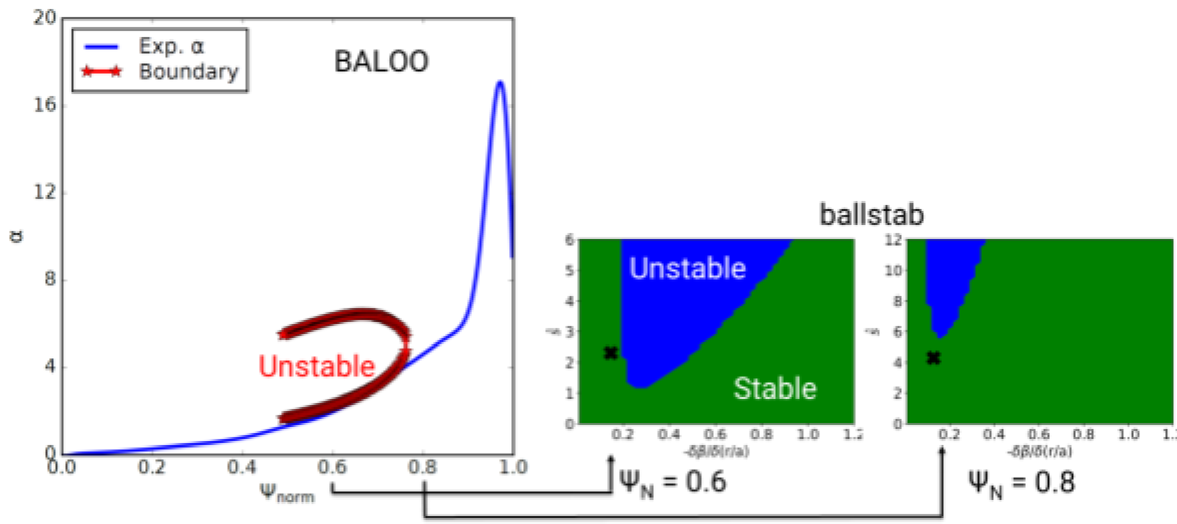

Figure 3: BALOO and ballstab infinite-*n* ballooning stability for RUN2.

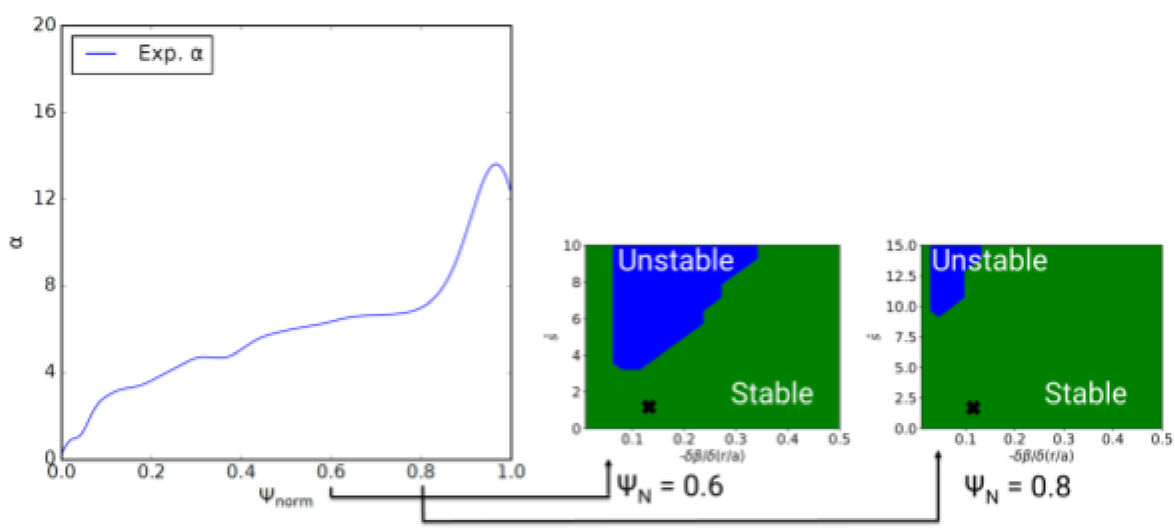

Figure 4: BALOO and ballstab infinite-*n* ballooning stability for RUN22.

Finite n ballooning mode stability with M3D-C1

A candidate ST-E1 equilibrium was assessed with the M3D-C1 code for ballooning mode stability. It was determined that the equilibrium was MHD stable to $n = 1$ to 9 modes. Then, in order to determine at which toroidal field the given pressure and current distribution *would* be unstable, the equilibria were "Bateman scaled", which keeps the current density fixed but varies the toroidal field to generate a family of equilibria. It was found that a field on the order of one half was required for instability. The mode structures of n = 1, 3, 5, 7, and 9 are shown in Fig. 5 with a Bateman scaling of 0.44. Growth rates for these modes were on the order of 6 - 20% of the Alfven time, and did not vary too significantly with either a finer mesh or including ideal or Spitzer resistivity.

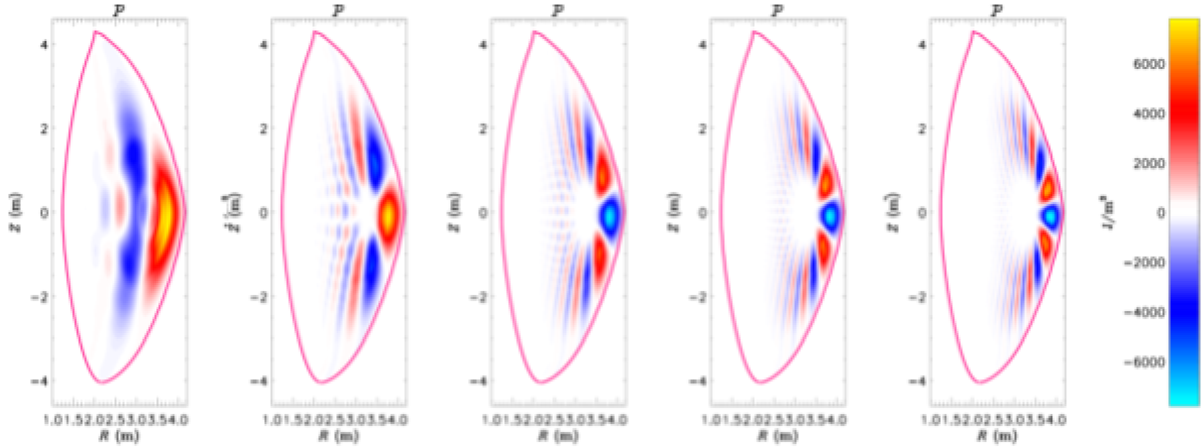

Figure 5: n = 1, 3, 5, 7, and 9 mode structures calculated with M3D-C1 for ST-E1 with Bateman scaling 0.44.

Radiated power assessment

This work was performed primarily by Jack Berkery and Kajal Shah from PPPL.

A new module being developed at PPPL called the Power Radiation Analysis Module (PRAM) was tested on an ST-E1 equilibrium. The module includes atomic data and gives a one or two dimensional estimate of the radiated power given an input electron density and temperature profile, as well as impurity profiles. For this ST-E1 case, both helium and lithium were considered, with concentrations of n_{He}/n_e = 3.1% and n_{Li}/n_e = 2.3%. This led to radiated powers of 1.1 and 1.9 MW, respectively, which compared to about 7 MW from the hydrogenic species and about 2.4 MW from synchrotron radiation. Figure 6 shows the two dimensional radiated power density from the impurities.

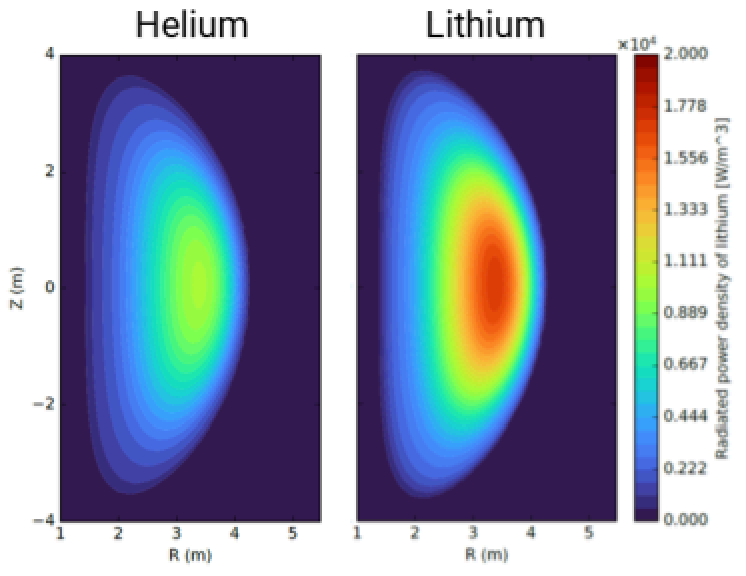

Figure 6: Radiated power contours from helium and lithium for an ST-E1 case.

Mapping Gyrokinetic-Constrained Burning Plasmas Across Shaping and Aspect-Ratio

This work was performed primarily by Jason Parisi from PPPL.

In this work package, gyrokinetic stability was evaluated for a range of equilibria. The main goal was to characterize the strength of micro-stability across a range of target equilibria, primarily scanning in aspect-ratio and magnetic field strength. In addition to these two parameters, we extended the scan to include two more shaping parameters: triangularity and squareness.

Initially, there were several iterations of a basecase ST-E1 equilibrium to find ideal-ballooning stable profiles. While we eventually found ideal-ballooning stable profiles, there were many other microinstabilities such as kinetic-ballooning-modes (KBMs), microtearing modes (MTMs), trapped-electron-modes (TEMs), and electron-temperature-instability (ETG) modes, as shown in Figure 7. This prevalence of TEM is important because many studies report neoclassical ion thermal transport in spherical tokamaks, which is not what we find here.

Due to the prevalence of KBM instability, we designed a coupled gyrokinetic and equilibrium optimizer that adjusted the equilibrium and profiles to stabilize the KBM by bringing the equilibrium below the KBM's first stability boundary.

After obtaining equilibria that are KBM stable, we use the transport codes TGYRO and TRINITY to determine the self-consistent profiles for a given equilibrium and the fusion power output for a given heating source, giving the plasma gain Q. Because of the difficulty of obtaining converged nonlinear simulations with fast-growing KBMs, the linear optimization was performed before the nonlinear transport simulations.

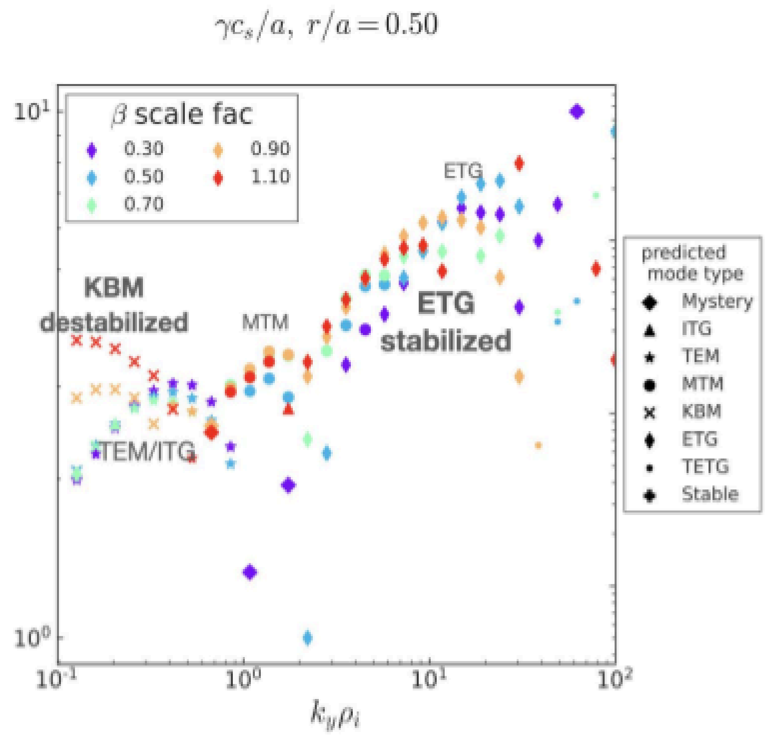

Figure 7: Gyrokinetic growth rates (y-axis) across a range of binormal wavenumbers (x) for an un-optimized ST-E1 equilibrium at r/a = 0.5. The equilibrium beta has been scanned to find proximity to instability. Simulations performed using CGYRO.

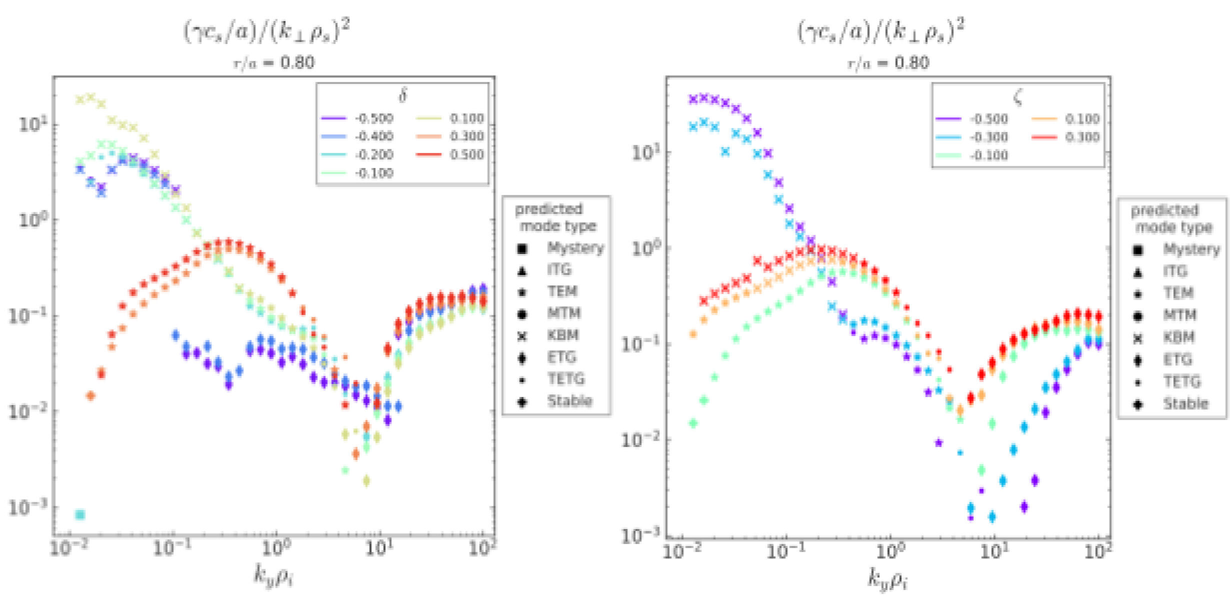

Figure 8: Effect of triangularity (left) and squareness (right) on the quasilinear diffusion estimate from gyrokinetic simulations at r/a = 0.8. Simulations performed using GS2.

In Figs 8-10, we plot the quasilinear diffusion coefficient $\gamma/k_{\perp}^{2}$ obtained from gyrokinetic simulations for equilibria with different triangularity, squareness, field-strength, and aspect-ratio. Notably, KBMs are driven more strongly with decreasing triangularity, decreasing squareness, lower toroidal field, and lower aspect-ratio. Curiously, both higher triangularity, higher squareness, higher toroidal field, and higher aspect-ratio are predicted to drive higher transport across all wavenumbers, with the exception of the KBM. Given that KBM instability typically appears at the plasma edge, a self-consistent pedestal solution, which is not present, is required to determine definitively the effect of these parameters on plasma transport, and therefore fusion power and plasma gain. In Fig 11, we plot several gyrokinetic quantities versus wavenumber and radius for the aspect-ratio = 1.9 case (run 09).

It is also worth noting that we have scanned these parameters individually. A more systematic approach would involve varying each of these parameters without holding other parameters fixed.

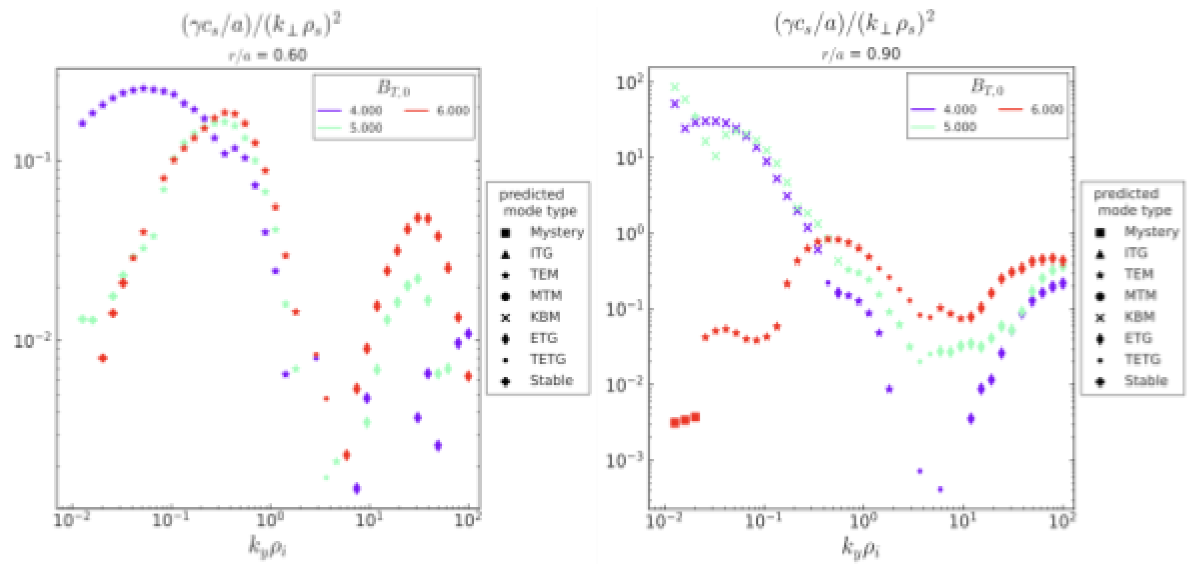

Figure 9: Effect of toroidal magnetic field strength on the quasilinear diffusion estimate from gyrokinetic simulations at r/a = 0.60 (left) and r/a = 0.90 (right). Simulations performed using GS2.

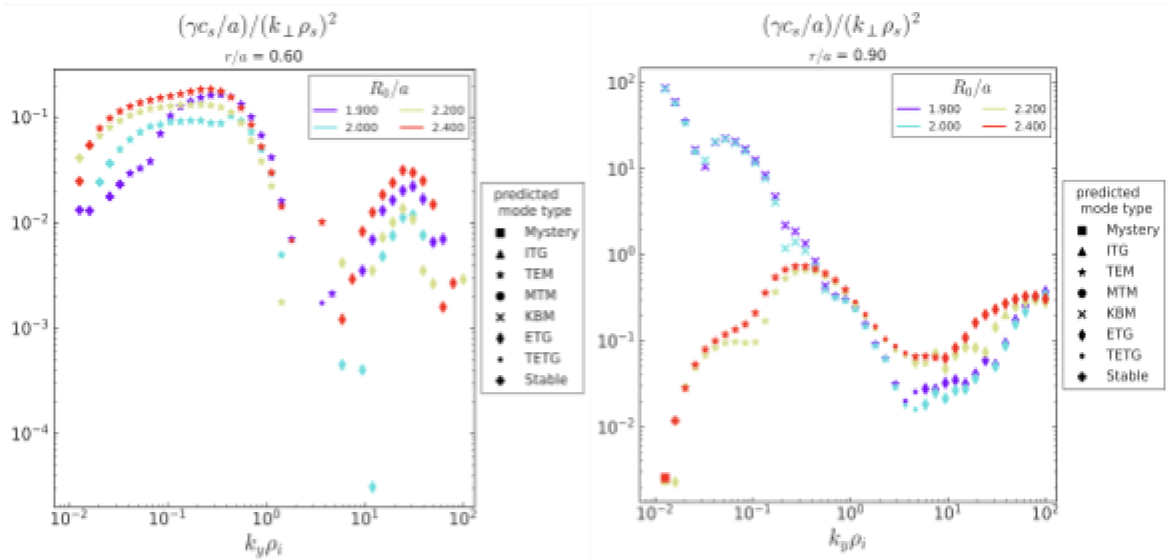

Figure 10: Effect of aspect-ratio on the quasilinear diffusion estimate from gyrokinetic simulations at r/a = 0.60 (left) and r/a = 0.90 (right). Simulations performed using GS2.

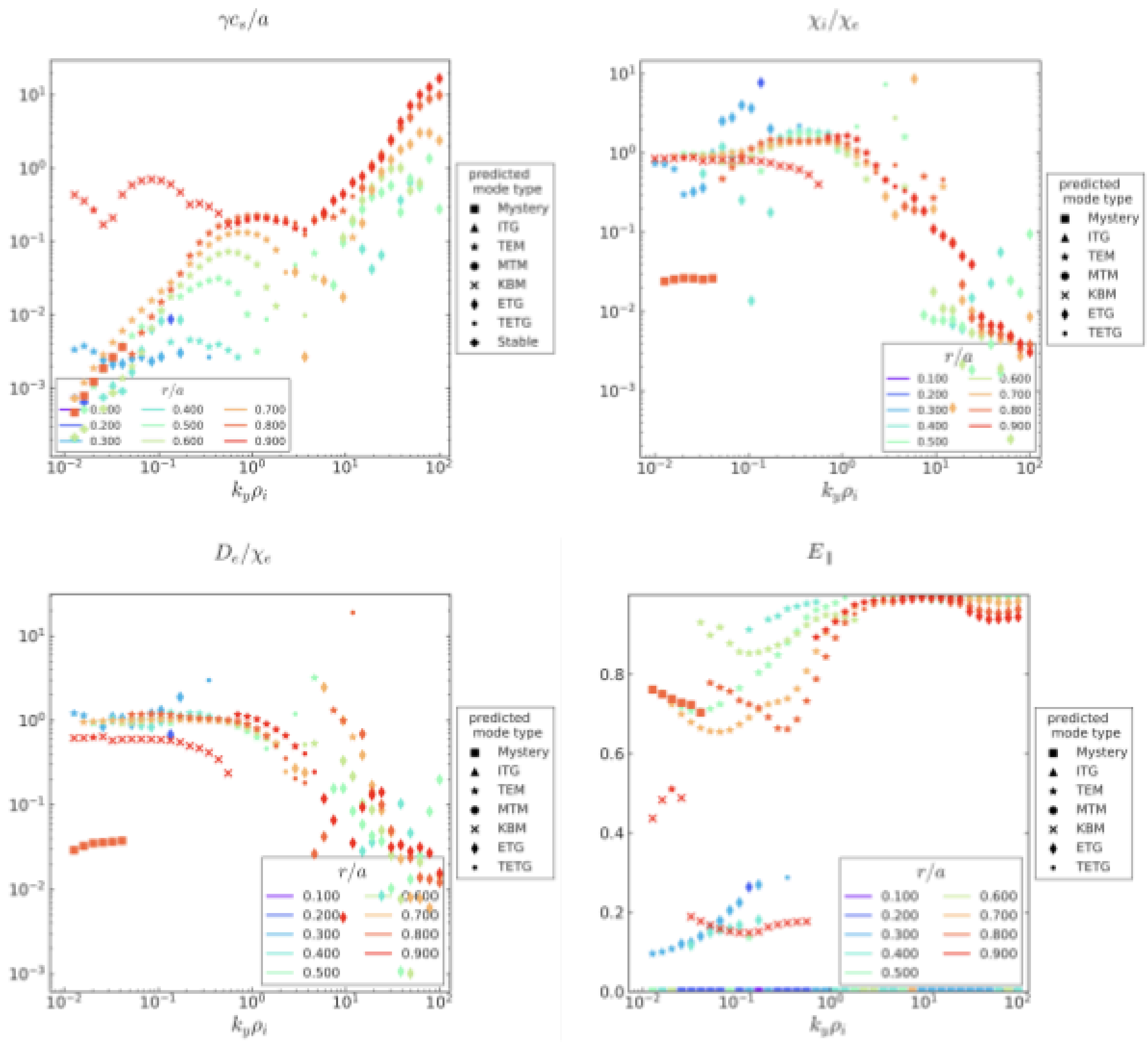

Figure 11: Linear growth rate (top left), ratio of main ion to electron heat diffusivity (top right), ratio of electron particle to heat diffusivity (bottom left), and normalized parallel electric field (bottom right) for run 09 with aspect-ratio = 1.9

Geometric burn control

This work was performed primarily by Jason Parisi from PPPL.

While investigating the effect of various plasma shaping parameters on KBM stability, an intriguing feature was noticed and further explored. It was determined that the total fusion power could be controlled by adjusting the plasma volume fraction that is packed into power dense regions. Using an example ST-E1 burning plasma, by modifying the plasma edge squareness the total fusion power was seen to be doubled at almost constant total plasma volume and fusion power density. Therefore, increased plasma squareness could be extremely beneficial to a fusion reactor and squareness control could be desirable for power load balancing. This effect is illustrated in Fig. 12, where the total fusion power was found to be 215, 311, and 403 MW for the squareness levels of -0.15, -0.03, and 0.03, respectively.

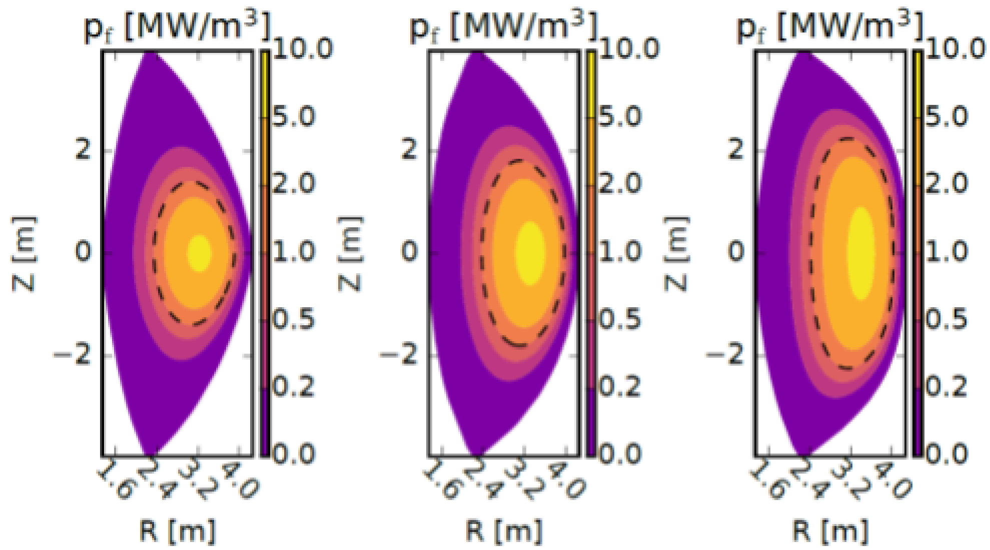

(a) $\zeta_0 = -0.15$ (b) $\zeta_0 = -0.03$ (c) $\zeta_0 = 0.03$

Figure 12: squareness scan, showing fusion power density.

Subject Inventions

None

Publications and Presentations

“Geometric Burn Control for Tokamaks” by J. Parisi et al was presented as a poster at the INFUSE workshop at PPPL on February 27-28, 2024, at the Institute for Fusion Studies at UT Austin on March 26, 2024. It was submitted to Physical Review Letters on April 17, 2024, and a preprint can be found on arXiv: https://arxiv.org/abs/2404.04387.

“Mapping Gyrokinetic-Constrained Burning Plasmas Across Shaping and Aspect-Ratio” by J. Parisi et al is in preparation and will be submitted to Nuclear Fusion as an article after clearing internal peer review at Princeton Plasma Physics Laboratory and Tokamak Energy.